



## Effect of overhang structures on the roughness, porosity, and microstructure of L-PBF printed Ti-6Al-4V alloys

The development of additive manufacturing (AM) has allowed for increased flexibility and complexity of designs over formative and subtractive manufacturing. However, geometric feature such as overhangs, affect the as-built microstructure, roughness, and porosity. This work examines the effect of varying laser energy has on the porosity, roughness, and microstructure of overhang structures.

J. Power<sup>a</sup>, M. Hartnett<sup>b</sup>, O. Humphreys<sup>a</sup>, D. Egan<sup>a</sup>, and D.P. Dowling<sup>a</sup>

<sup>a</sup>I-Form Centre, School of Mechanical and Materials Engineering, UCD, Belfield, Dublin 4, <sup>b</sup>Irish Manufacturing Research, Block A, Collegeland, Rathcoole, Co. Dublin, D24 WC04

### Introduction

Overhang structures present an issue for Laser- Powder Bed Fusion (L-PBF), due to melt pool overheating which can occur due to the lower thermal conductivity of the powder layer below the overhang, compared with the bulk metal (Figure 1). In this investigation the effect of varying the laser energy conditions during the printing of Ti-6Al-4V alloy parts were investigated. Laser energies were varied as detailed in table 1, while the porosity and roughness of the resulting overhang structure was evaluated using micro-CT analysis.

### Porosity & Roughness

Underheating caused pores to form laterally of the overhang region, likely due to spatter. The level of overhang roughness (Ra), exhibited a direct correlation with the level of melt pool energy based on photodiode (LaserVIEW) measurements. With increased overhang roughness with the higher melt pool temperatures associated with increased laser energy. This study demonstrated that the overhang melt pool temperature should be closer to the bulk regions melt pools to reduce the roughness and porosity (Figure 2).

Part ID	Laser Energy (J)			
	Layer 1	Layer 2	Layer 3	Layer 4
1	8312.5	10000	10000	10000
2	8312.5	10000	10000	10000
3	7600	10000	10000	10000
4	7600	10000	10000	10000
5	6400	10000	10000	10000
6	281.5	439.8	687.2	1073.7
7	4401.3	4876.7	5403.6	5987.4
8	1180.7	1542.1	2014.2	2630.8
9	163.0	214.5	282.2	371.3
10	47.5	67.8	96.9	138.4
11	2146.4	2378.3	2635.2	2919.9
12	47.5	67.8	96.9	138.4
13	163.0	214.5	282.2	371.3

Table 1: Laser print parameters used for the first four layers of each sample

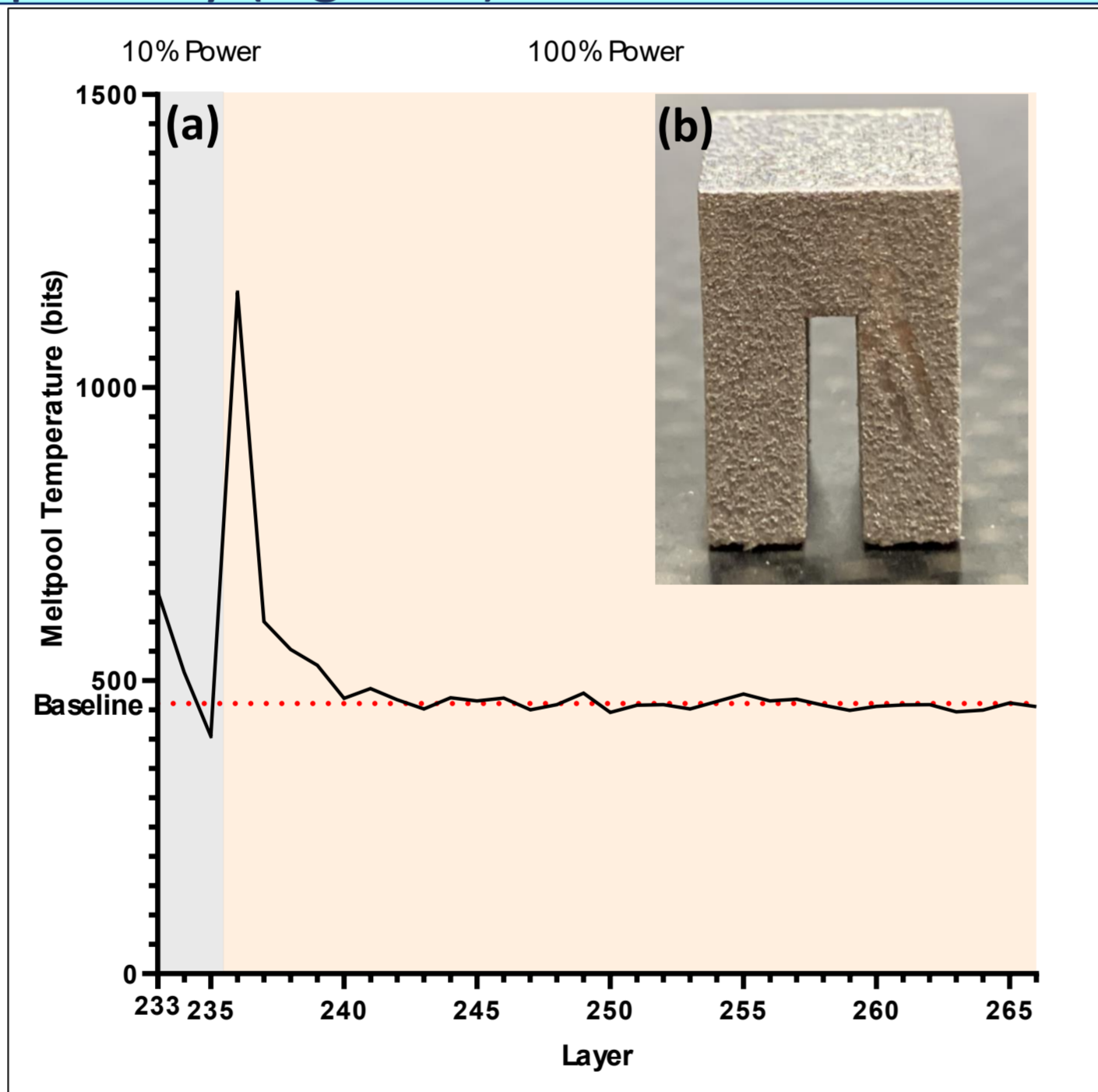


Figure 1: (a) Melt pool temperature (bits) measured in-situ using an IR sensor. A large increase in the overhang melt pool temperature is detected after the first overhang layer is printed. (b) An overhang print test sample from this study.

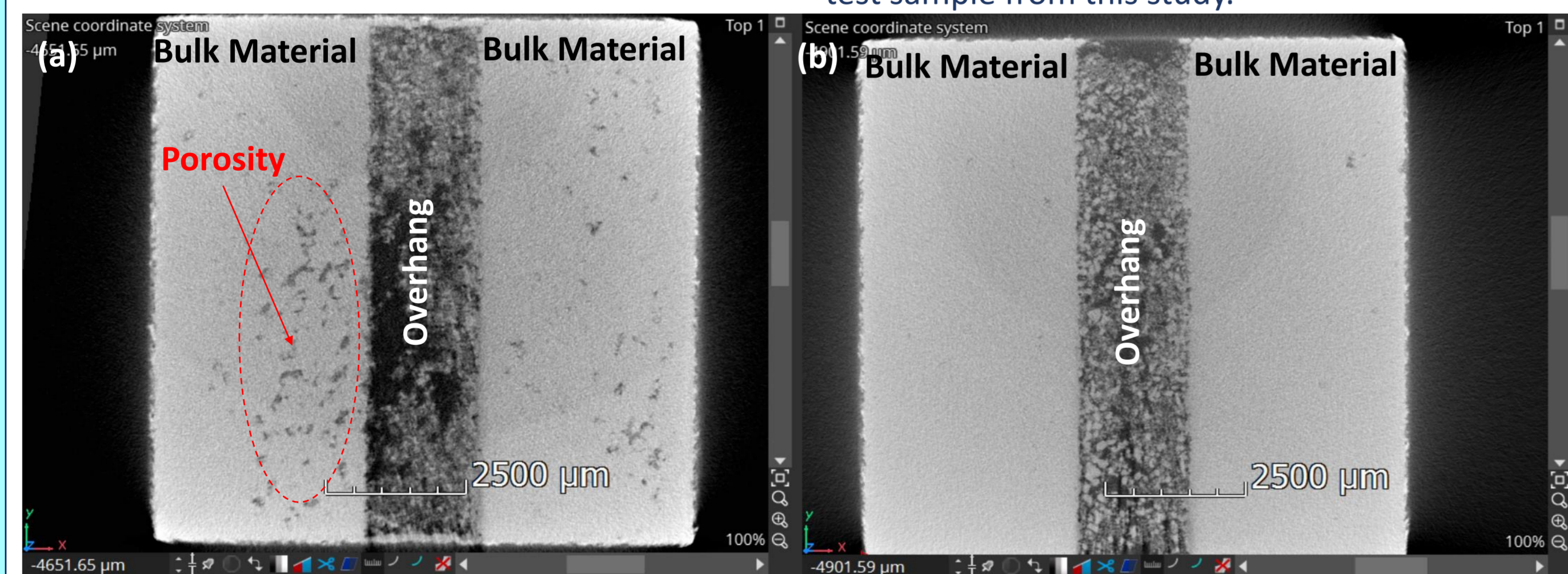


Figure 2: Plan (top) view of the overhang μCT scan. Increased porosity is present under underheating conditions, inside the red circle (a) printed at 5.0 standard deviations below nominal temperature (b) sample with low porosity printed at 8.4 standard deviations above nominal temperature.

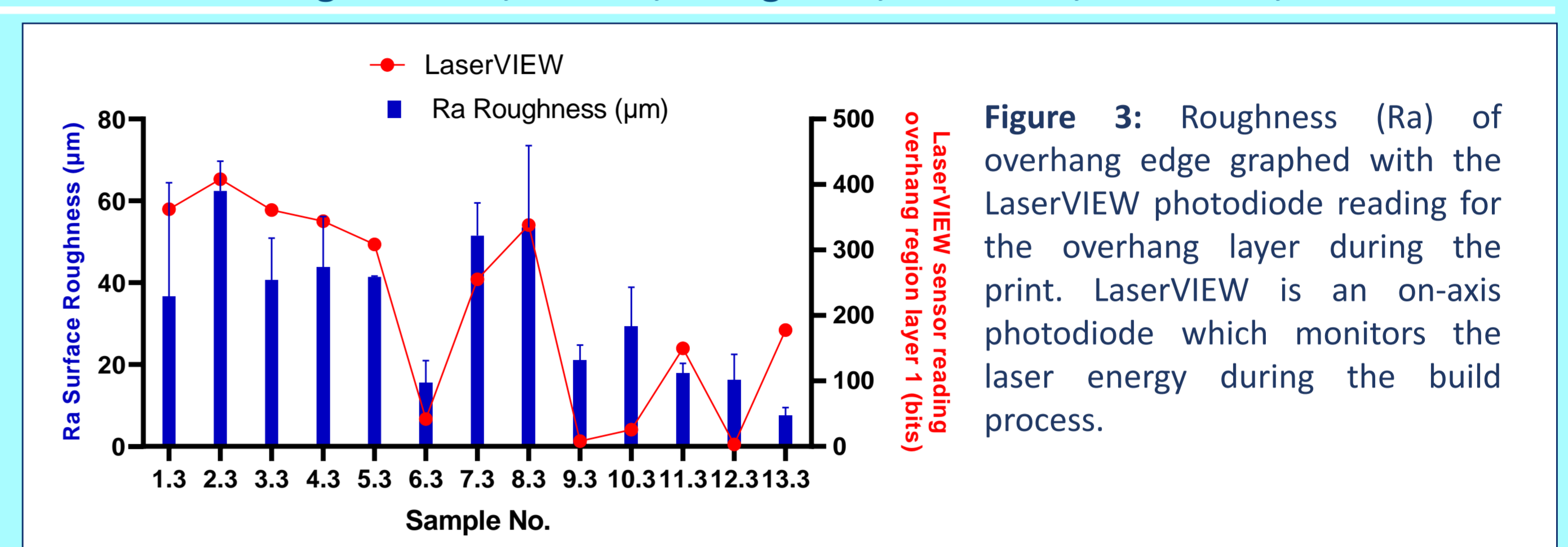


Figure 3: Roughness (Ra) of overhang edge graphed with the LaserVIEW photodiode reading for the overhang layer during the print. LaserVIEW is an on-axis photodiode which monitors the laser energy during the build process.

### Microstructure

Optical microscopy of the overhang samples revealed the formation of  $\alpha$  colonies in the print layers above the overhang. The size of these  $\alpha$  colonies varied from  $17.9 \pm 6.7 \mu\text{m}$  to  $28.9 \pm 10.2 \mu\text{m}$  and were found within  $100 \mu\text{m}$  of the overhang edge. SEM imaging of the samples showed that the  $\alpha'$  needles were shorter and narrower in the overhang region of the samples, which were printed using lower laser power (Figures 4 & 5). Previous research has established a link between shorter  $\alpha'$  needle morphology and lower laser power. Annealing may have also occurred due to the higher melt pool temperatures.

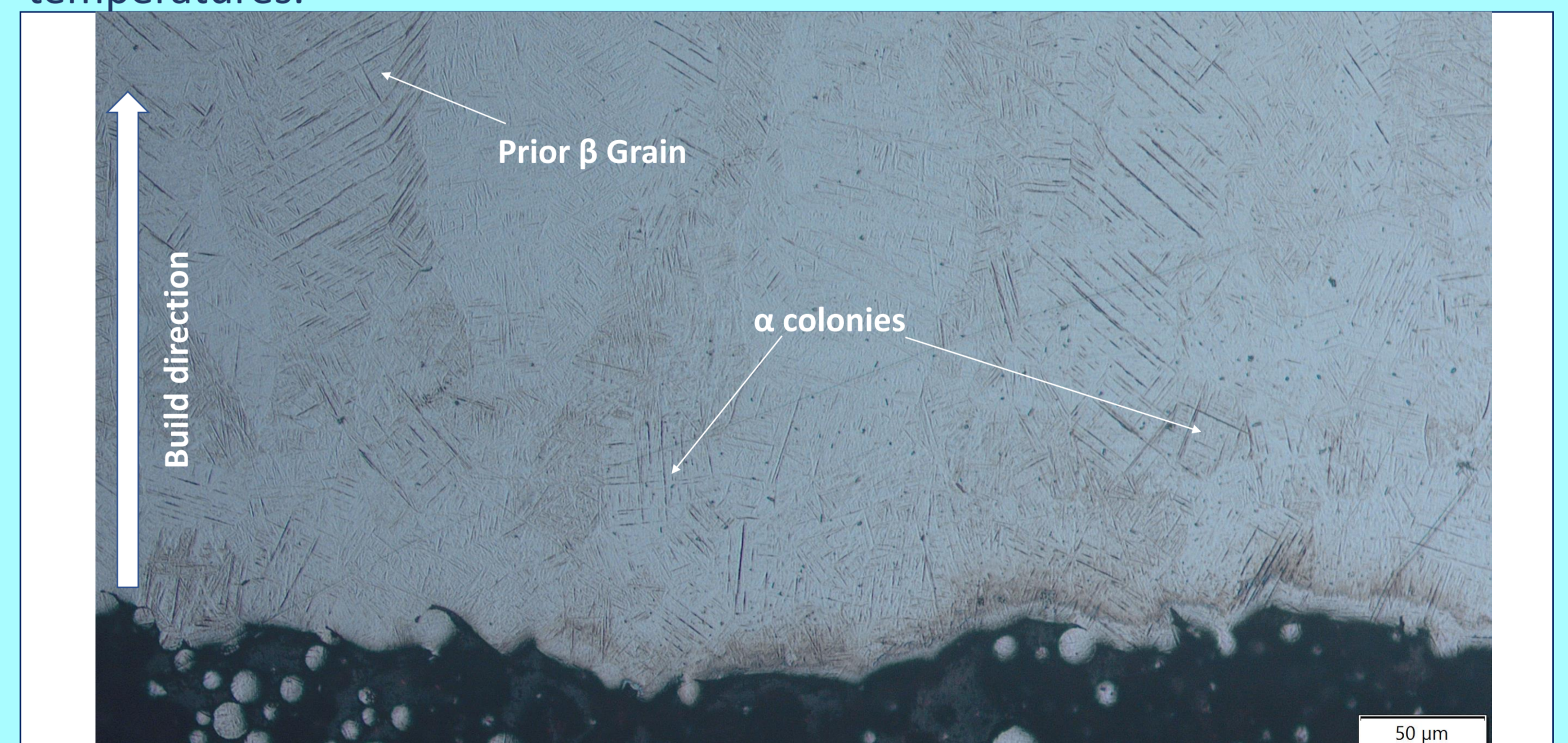


Figure 4: Optical microscopic image of overhang sample at 10X magnification. Formation of  $\alpha$  colonies dominates the layers printed above the overhang.

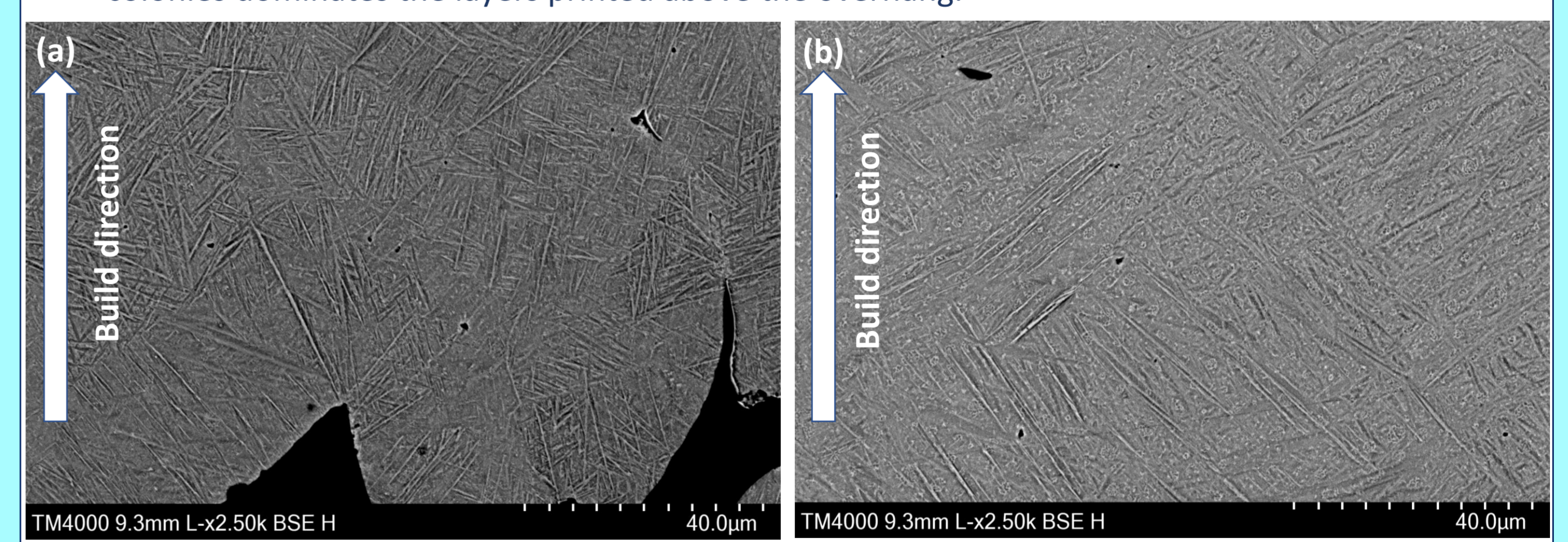


Figure 5: SEM images of overhang sample at 2,500X magnification. Image (a) area directly above overhang exhibits shorter and narrower  $\alpha'$  needles. Image (b) shows the print area further above the overhang, showing  $\alpha'$  needles which are longer and thicker with a 'basket weave' configuration.

## CONCLUSION

Overhang structures in printed alloy structures can create difficulties due to variations in the melt pool temperature, due to decreased thermal conductivity of the powder immediately below the print layer. By controlling the laser energy during the printing of L-PBF overhang structures, the level of porosity and roughness can be significantly reduced (an 88% reduction in Ra roughness was achieved), while the microstructure can be optimised. This is achieved based on closely monitoring the melt pool temperature during overhang printing (photodiode measurements). Informed by these measurements the laser treatment energy is closely controlled to prevent over/underheating of the overhang print layers.